Cement analysis by X-ray diffractometry

Atsushi Ohbuchi* and Takahiro Kuzumaki**

1. Introduction

Cement is used as a raw material in the construction of buildings[1], tunnels[2], dams[3], and bridges[4]. Basically, cement consists of clinker, calcium sulfate hydrate as a plaster component, aggregate, and water (Fig. 1)[5]. The hardening process of cement proceeds by a hydration reaction of components in cement, and some hydrate components—ettringite (AFt, $3CaO \cdot Al_2O_3 \cdot 3CaSO_4 \cdot 32H_2O$), monosulfate (AFm, $3CaO \cdot Al_2O_3 \cdot CaSO_4 \cdot 12H_2O$), monocarbonate (AFmc, $3CaO \cdot Al_2O_3 \cdot CaCO_3 \cdot 11H_2O$), and C–S–H—are formed. Clinker, which is a raw material of cement, is produced from limestone via a calcination process, and it is composed of alite (C_3S: $3CaO \cdot SiO_2$), belite (C_2S: $2CaO \cdot SiO_2$), aluminate (C_3A: $3CaO \cdot Al_2O_3$), and ferrite (C_4AF: $4CaO \cdot Al_2O_3 \cdot Fe_2O_3$)) as major components (Fig. 2)[5]. The four major components have different characteristics of time for hardening and strengthening of the cement (Table 1)[5]; for example, alite strengthens in a short period whereas belite strengthens over a long period. Therefore, the composition of the four major components in the clinker is changed for various construction types since cement is used for a wide variety of purposes.

Ordinary Portland cement is a popular cement. The hardening speed of high early strength Portland cement with high alite concentration is much faster than for ordinary Portland cement. High early strength Portland cement is used as emergency construction concrete and winter concrete. A moderate heat Portland cement, which is used for making dams, with low heat of hydration, has a large concentration of belite. Therefore, composition analysis of clinker and cement is needed because many kinds of cements are required for various construction situations.

Clinker composition has been analyzed by scanning electron microscopy (SEM)[6]. Major components in the clinker are classified by observing their shape with SEM and their concentration is calculated by point counting analysis, although this method takes a long time and needs analyst skill. Also, the Bogue calculation[7] is used to calculate composition of the four major components in clinker from elemental composition. However, composition by the Bogue calculation shows differences with the actual composition of clinker. Composition of cement is evaluated by elemental analysis using X-ray fluorescence spectrometry (XRF)[8] based on ASTM C114[9]. On the other hand, X-ray diffraction (XRD), a rapid analysis method for crystalline phases, can be applied to identify components of clinker and cement[10]

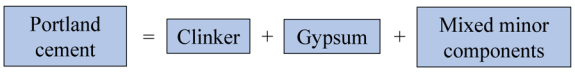

Fig. 1. Composition of Portland cement[5].

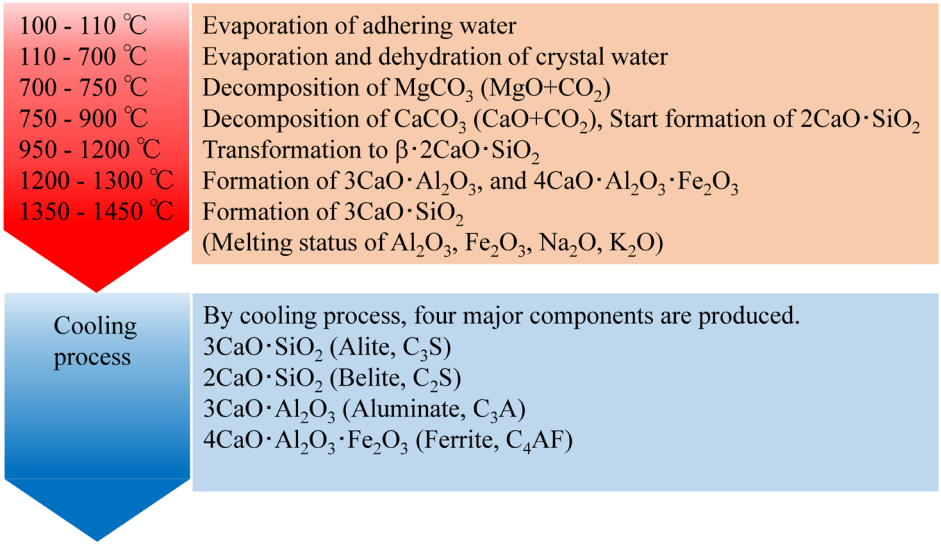

Fig. 2. Chemical change of clinker by calcination process[5].

* Rigaku Americas Corporation.
** Application Laboratories, Rigaku Corporation.

Table 1. Characteristics of the major four components in clinker[5].

Characteristic		Alite (C_3S)	Belite (C_2S)	Aluminate (C_3A)	Ferrite (C_4AF)
Strength development	Short term	High	Low	High	Low
	Long term	High	High	Low	Low
Heat of hydration		Medium	Low	High	Low

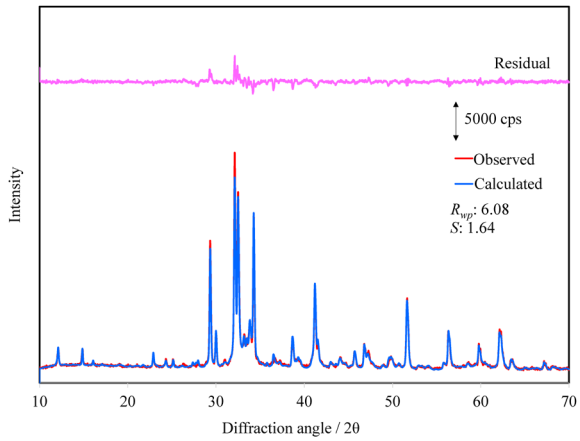

Fig. 3. Observed (red line) and calculated (blue line) diffraction patterns and residual (pink line) after Rietveld refinement of NIST 2688 SRM.

Table 2. Quantitative result of four major components in NIST 2688 SRM by Rietveld refinement.

Component	mass%	
	Analytical value	Certified value
Alite (C_3S)	65.2 (0.2)	64.95±1.04
Belite (C_2S)	17.3 (0.3)	17.45±0.96
Aluminate (C_3A)	4.52 (0.14)	4.99±0.50
Ferrite (C_4AF)	12.98 (0.14)	12.20±0.84

Parenthesis: Standard deviation of 1σ

in addition to quantitative analysis by Rietveld refinement[11] because the four major components are contained in clinker as crystalline phases. In this paper, XRD was applied to cement analysis and some applications are introduced.

2. Quantification by Rietveld Refinement

2.1. Major component analysis

The four major components in NIST clinker SRM were analyzed by Rietveld refinement because most their diffraction peaks in clinker are overlapped and the calibration curve method was not applicable as a quantitative method. Rietveld refinement was applied over the entire diffraction profile (e.g., 5–90°/2θ). In the past, data for Rietveld refinement required a long measurement time (e.g., overnight) with laboratory apparatus due to the low count rate of scintillation counters. Recently, data for Rietveld refinement can be acquired more quickly (e.g., 1 hour) using laboratory apparatus due to the development of semiconductor detectors. NIST SRM clinker was analyzed in 10 minutes using the one-dimensional silicon strip detector D/teX Ultra250. The Rietveld refinement was performed using the SmartLab Studio II program, which is based on the Rietveld method. The background for each pattern was defined as the interpolation of n points that were introduced manually. The profile function used was a split pseudo-Voigt function[12] to take into account the asymmetry of each peak. Crystal structure data for the four major components (alite, belite, aluminate, and ferrite) in the qualitative analysis were taken from the ICSD database. The thermal vibration parameters and atomic positions were fixed during refinement. The parameters optimized were: background coefficients, peak shift, lattice constant, profile parameters, and preferred orientation. Quantitative values for each crystalline phase were calculated by the following equation:

$$W_i = \frac{(S_i Z_i M_i V_i)}{(\sum_j S_j Z_j M_j V_j)} \quad (1)$$

In Equation (1), W_i is the weight fraction of the analyte component i, S is the scale factor after Rietveld refinement, Z is the number of molecules within a unit cell, M is the molecular weight, and V is the volume of the unit cell derived from the lattice constants. Analytical results and quantitative values for NIST 2688 SRM are shown in Fig. 3 and Table 2. Residuals between observed and calculated profiles were small, and R_{wp} and S indications of Rietveld refinement had small values. Additionally, the analytical values of the four major components were in good agreement with certified values.

2.2. Cement analysis

Rietveld refinement was applied to several cements obtained from three countries. Figure 4 shows diffraction patterns of the three cement materials. The diffraction patterns were different, especially in the sections enclosed in boxes. Quantification result by Rietveld refinement of the components in the three cement materials is shown in Table 3. Eight components were identified in A cement, 9 components in B cement, and 11 components in C cement. Sulfate (anhydrite ($CaSO_4$), basanite ($Ca(SO_4)(H_2O)_{0.5}$), or gypsum ($Ca(SO_4)(H_2O)_2$)) is related to the hardening process of cement, and sulfate components were contained in all cement materials. Also, portlandite ($Ca(OH)_2$) was

contained in all cement materials. It is considered that free-lime (CaO) in all cement materials was transformed to portlandite due to reaction with moisture in the environment. Ferrite concentration in B cement was lower than the other two cement materials, and arcanite (α-K_2SO_4) was identified in only B cement as a residue of raw material. Belite concentration in C cement was higher than the other two cement materials. Additionally, C_2S-$\alpha'H$ was contained in only C cement. C_2S-$\alpha'H$ is produced between about 1200 to 1400℃ during the calcination process. It is considered that C_2S-$\alpha'H$ remained in C cement due to a different heating or cooling process compared to the other two cement materials. The four major components in A and B cement had a different composition from C cement. On the other hand, the hardening speed of A and B cement would be different compared to C cement.

2.3. Amorphous analysis

Blast furnace slag (BFS) is an amorphous phase additive agent used to form a fine and stable curing composition. Portlandite blast-furnace cement mixed with blast furnace slag is used for making dams and in construction at docks and harbors due to its seawater resistance and chemical resistivity arising from characteristics of high long-term strength improvement. In XRD, an amorphous phase can be determined by Rietveld refinement with the internal standard method[13], which can be applied to cement[14), (15]. The weight fraction calculated by Equation (1) is converted to the concentration of the amorphous phase by the following equations from the internal standard method.

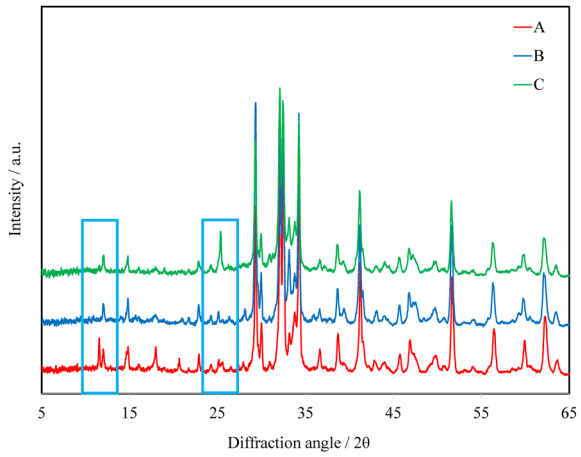

Fig. 4. Diffraction patterns of three cement materials.

$$C_j = \frac{W_i \times 100}{C'_{STD}} \times C_{STD} \tag{2}$$

$$C_A = 100 - C_{STD} - \sum C'_j \tag{3}$$

In Equation (2) and (3), C_A is residual content including the amorphous phase (mass%), C_{STD} is the concentration of the internal standard (mass%), C'_{STD} is the calculated concentration of the internal standard analyzed by Rietveld refinement (mass%), C_j is the quantitative value of crystalline phase j corrected by the internal standard material (mass%), and $\sum C'_j$ is the total quantitative value of each crystalline phase (mass%). Corundum (α-Al_2O_3) is typically used as an internal standard material because it is not contained in cement and is a stable material at ordinary temperature and normal pressure. However, the internal standard method takes time because a certain concentration of corundum, for example 10 or 20 mass%[13], must be mixed into the cement. The Reference Intensity Ratio (RIR) method[16] is the simplest method for quantitative analysis, and the RIR value is used for quantitative analysis of amorphous phases in addition to crystalline phases without mixing internal standard materials into the sample or requiring

Table 3. Quantitative result of components in three cement materials by Rietveld refinement.

Component	mass%		
	A cement	B cement	C cement
Alite (C_3S)	69.7 (0.4)	67.5 (0.4)	60.3 (0.4)
Belite (C_2S)	7.8 (0.4)	8.9 (0.4)	15.3 (0.4)
Belite (C_2S-α'_H)	—	—	2.21 (0.12)
Aluminate (C_3A)	2.73 (0.08)	5.81 (0.09)	3.40 (0.08)
Ferrite (C_4AF)	10.70 (0.18)	7.68 (0.18)	11.9 (0.2)
Calcite ($CaCO_3$)	—	4.13 (0.12)	1.61 (0.15)
Anhydrite ($CaSO_4$)	—	—	3.78 (0.1)
Bassanite ($Ca(SO_4)(H_2O)_{0.5}$)	3.71 (0.14)	2.01 (0.09)	0.43 (0.09)
Gypsum ($Ca(SO_4)(H_2O)_2$)	2.13 (0.08)	—	0.022 (0.008)
Portlandite ($Ca(OH)_2$)	1.90 (0.08)	1.98 (0.17)	0.75 (0.11)
Periclase (MgO)	1.27 (0.06)	0.69 (0.06)	0.32 (0.05)
Arcanite (α-K_2SO_4)	—	1.26 (0.14)	—

Parenthesis: Standard deviation of 1σ

the preparation of a calibration curve. The RIR value is calculated as the intensity ratio of the analyte component and corundum mixed in equal amount. The weight fraction is calculated using Equation (4) by the RIR method.

$$W_i \propto \frac{I_i^{max}}{R_i} \tag{4}$$

W_i is the mass fraction of the analyte component i, I_i^{max} is the strongest intensity, R_i is the RIR value. The amorphous phase is determined by Equation (5) combined with Rietveld refinement.

$$W_A = \frac{S_A / R_A}{\sum S_j / R_j} \tag{5}$$

W_A is the weight fraction of the amorphous phase, S_A and S_j are scale factors calculated by Rietveld refinement, and R_A and R_j are the RIR values.

To calculate the RIR value of an amorphous phase, a simulated sample was prepared mixing known concentrations of the components, including BFS[15]. An RIR value of 3.60 for BFS showed the smallest differences between known and measured concentrations, and this RIR value was applied to quantification of amorphous phases in cement. Table 4 shows analytical results of the amorphous phase in two cement samples by RIR method/Rietveld refinement. Concentrations of the amorphous phase were compared with results by the internal standard method using corundum. Concentrations of the amorphous phase in cement samples by RIR method showed good agreement with results by the internal standard method, as do crystalline phases except for calcite. Calcite has preferred orientation in the (104) direction that is corrected by the March–Dollase function[17] in Rietveld refinement. Correction for variation in X-ray diffraction intensity was difficult due to many overlapping diffraction peaks in the X-ray diffraction pattern of cement even if March–Dollase function was applied. Therefore, the RIR method can be applied to determine the amorphous phase effectively.

3. Free-Lime Analysis

Free-lime in clinker is a residue from the calcination process of limestone, and it is converted to calcium hydroxide (portlandite) via a hydration reaction due to the high hydroscopic property of free-lime. The hydration reaction of free-lime causes cracks in concrete due to volume expansion. Figure 5 shows variations in the diffraction pattern of free-lime under 30°C and 40% relative humidity environment by hydration process using an XRD-DSC system. Free-lime is transformed to portlandite after only 1 hour of reaction time because

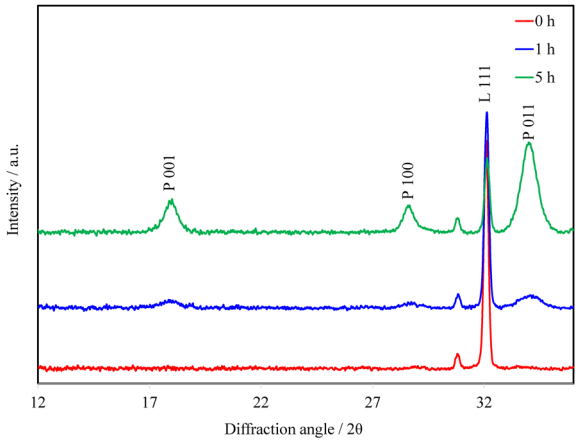

Fig. 5. Variation diffraction patterns of free-lime under 30°C and 40% relative humidity environment.
L: Lime (CaO), P: Portlandite ($Ca(OH)_2$)

Table 4. Quantitative result of crystalline and amorphous phases in instant and rapidly hardening cements by RIR/Rietveld refinement[15].

Component	Concentration/mass%			
	Instant cement		Rapidly hardening cement	
	RIR method	Internal standard method	RIR method	Internal standard method
Calcite ($CaCO_3$)	52.4	56.3	56.1	53.5
Alite (C_3S: $Ca_3(SiO_4)O$)	19.6	14.2	13.9	13.1
Belite (C_2S: $Ca_2(SiO_4)$)	3.03	3.80	1.30	3.17
Aluminate (C_3A: $Ca_9(Al_2O_6)_3$)	1.01	1.18	1.11	1.87
Ferrite (C_4AF: $Ca_2(AlFeO_5)$)	1.89	1.91	1.64	1.66
Quartz (α-SiO_2)	1.98	2.13	1.68	1.17
Dolomite ($CaMg(CO_3)_2$)	2.71	4.30	2.28	3.15
Anhydrite ($CaSO_4$)	—	—	2.02	1.43
Bassanite ($Ca(SO_4)(H_2O)_{0.5}$)	—	—	1.09	1.68
Gypsum ($Ca(SO_4)(H_2O)_2$)	0.90	0.52	—	—
Amorphous	16.5	15.6	18.9	19.2

free-lime has extremely high reactivity with water. Therefore, quick quantification analysis of free-lime in clinker or cement is needed. There are some analytical methods of free-lime; in particular, free-lime analysis is defined as JCAS I-01[18] issued by Japanese Cement Association Standard in Japan. In JCAS I-01, free-lime is analyzed by a titration method using ethylene glycol or glycerin. On the other hand, XRD can be applied to the quantification of free-lime. For example, a calibration curve is used for the determination of free lime as an empirical method (Fig. 6). Also, free-lime can be determined using a calibration curve method combined with elemental composition by simultaneous XRF spectrometry[19]. In addition to the calibration curve method, free-lime is determined by Rietveld refinement. Free-lime was produced from portlandite heated at 1000℃ for 5 hours and added to NIST 2687 SRM. Rietveld refinement was executed. Figure 7 shows the results of Rietveld refinement for NIST 2687 SRM added free-lime. Residuals between observed and calculated profiles were small, and R_{wp} and S indications of Rietveld refinement were low. Quantitative values are shown in Table 5, and quantitative and preparation values of free lime showed good agreement, as well as major components.

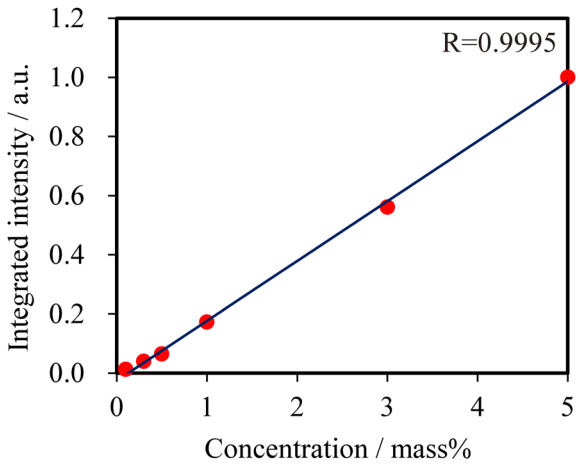

Fig. 6. Calibration curve of free-lime.

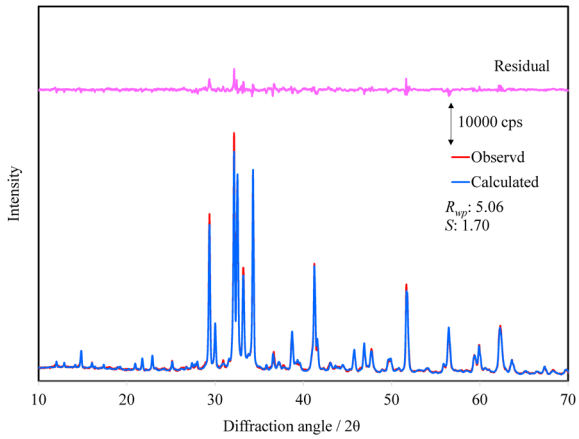

Fig. 7. Observed (red line) and calculated (blue line) diffraction patterns and residuals (pink line) after Rietveld refinement of NIST 2687 SRM added 0.5 mass% of free-lime.

Table 5. Quantitative result of major components and free-lime in NIST 2687 SRM by Rietveld refinement.

Component	mass%	
	Analytical value	Certified value
Alite (C_3S: $Ca_3(SiO_4)O$)	71.7 (0.3)	71.24±1.27
Belite (C_2S: $Ca_2(SiO_4)$)	12.8 (0.3)	12.57±1.22
Aluminate (C_3A: $Ca_9(Al_2O_6)_3$)	12.19 (0.9)	11.82±1.03
Ferrite (C_4AF: $Ca_2(AlFeO_5)$)	2.55 (0.08)	2.81±0.68
Arcanite (K_2SO_4)	0.24 (0.08)	0.92±0.15
Free-lime (CaO)	0.47 (0.06)	0.52*

Parenthesis: Standard deviation of 1σ

* Preparation value

4. Observation of Curing Process in the Rapidly Hardening Cement

A curing process of commercially available rapidly hardening cement was observed. Figure 8 shows identification result of crystalline phases in a rapidly hardening cement[10]. The rapidly hardening cement contained 10 components (alite, belite, ferrite, aluminate, calcite, dolomite, quartz, gypsum, anhydrite, and bassanite). Alite, belite, ferrite and aluminate were clinker components; calcite, dolomite, and quartz were aggregate components; gypsum, anhydrite, and bassanite were plaster components. Rietveld refinement was applied to the rapidly hardening cement. Alite concentration was highest of the four major components (Fig. 9). Referring to Table 1, the rapidly hardening cement had characteristics of short-term strengthening. Therefore, the hardening process of the rapidly

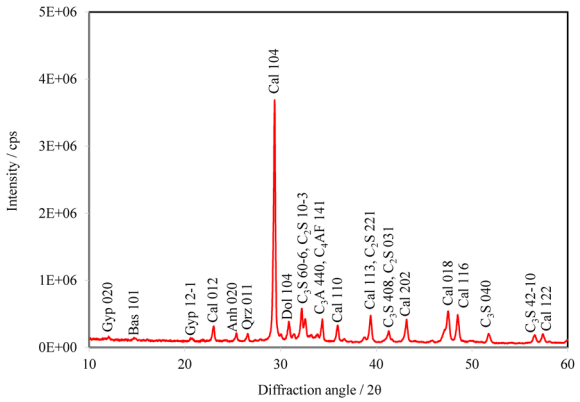

Fig. 8. Identification result of crystalline phases in rapidly hardening cement[10].

Anh: Anhydrite ($CaSO_4$), Bas: Bassanite ($Ca(SO_4)(H_2O)_{0.5}$), Cal: Calcite ($CaCO_3$), C_3A: Aluminate ($Ca_9(Al_2O_6)_3$), C_4AF: Ferrite ($Ca_2(AlFeO_5)$), C_3S: Alite ($Ca_3(SiO_4)O$), C_2S: Belite ($Ca_2(SiO_4)$), Dol: Dolomite ($CaMg(CO_3)_2$), Gyp: Gypsum ($Ca(SO_4)(H_2O)_2$), Qrz: Quartz (α-SiO_2)

hardening cement was observed by dropping water onto the rapidly hardening cement. Figure 10 shows diffraction patterns of the rapidly hardening cement during the hardening process. Each diffraction pattern was obtained from a one-minute measurement using a D/tex Ultra250 detector. The diffraction peak of ettringite, which is related to the hardening process produced from aluminate, gypsum, and water, was clearly observed on the diffraction pattern after approximately 40–50 minutes, although it takes ettringite longer to form than the hardening process of the rapidly hardening cement. Also, the diffraction peak of ettringite is not clearly observed during the hardening process of normal cement due to its low concentration.

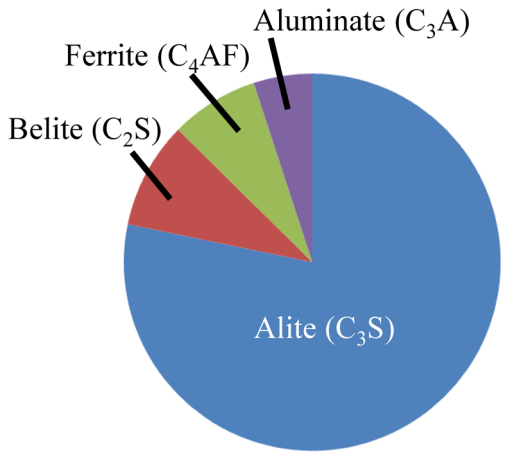

Fig. 9. Proportion of the four major components in rapidly hardening cement.

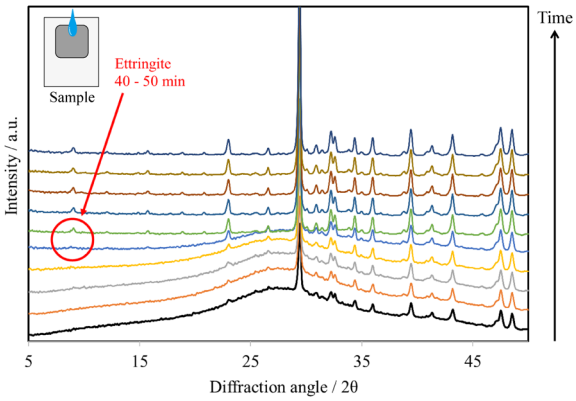

Fig. 10. Diffraction patterns collected during the calcification of rapidly hardening cement[10].

5. Collaboration Sample Holder between XRD and XRF

A pressed cement sample can be analyzed on both benchtop XRD and XRF instruments using a collaboration sample holder[20]. Figure 11 shows how the collaboration sample holder is used. A pressed sample is placed in the sample holder for XRF analysis and separate XRD analysis. Using the collaboration sample holder, the sample only has to be prepared once for both XRD and XRF analyses. The XRF result is used to estimate the scale factor of the four major components using the Bogue calculation in Rietveld refinement to obtain superior quantitative result for cement sample as follows.

$$C_3S=4.0701CaO-7.6024SiO_2-6.7187Al_2O_3-1.4297Fe_2O_3$$

$$C_2S=-3.0710CaO+8.6024SiO_2+5.0683Al_2O_3+1.0785Fe_2O_3=2.8675SiO_2-0.7544C_3S$$

$$C_3A=2.6504Al_2O_3-1.6920Fe_2O_3$$

$$C_4AF=3.0432Fe_2O_3$$

The scale factors, which are related to the quantitative values of the four major components, have to be estimated somehow. In Rietveld refinement, initial

Fig. 11. Configuration of the collaboration sample holder for benchtop XRD and XRF instruments.

Table 6. Quantitative values of the four major components in NIST 2688 SRM by Rietveld refinement combined with the Bogue calculation.

Component	mass%		
	Scale factors estimated from Bogue calculation	Using arbitrary initial scale factors	Certified value
Alite (C_3S)	64.2 (0.3)	72.3 (0.5)	64.95±1.04
Belite (C_2S)	18.2 (0.4)	12.4 (0.7)	17.45±0.96
Aluminate (C_3A)	5.26 (0.17)	4.0 (0.2)	4.99±0.50
Ferrite (C_4AF)	12.30 (0.17)	11.2 (0.3)	12.20±0.84

values of the scale factors are important to obtain accurate quantification result. Usually, an analytical program calculates each scale factor automatically; however, more accurate results are obtained when the scale factors of the four major components come from the Bogue calculation because these values have been shown to be close to the actual composition of the four major components. The scale factors were calculated automatically by the Bogue calculation via importing a CSV file of XRF results into the XRD software. The analytical result of the four major components in NIST 2688 SRM using scale factors estimated by the Bogue calculation and those fromarbitrary estimates are shown in Table 6. Quantitative values using the Bogue calculation were in good agreement with certified values compared to arbitrary estimation of scale factors. Analysts can obtain superior results without depending on detailed Rietveld refinement by using the Bogue calculation combination.

6. Conclusion

X-ray diffraction can be applied to major and minor components analysis as well as free-lime in cement material. Crystal polymorphs of major components are analyzed and quantitative values are obtained by Rietveld refinement. Measurement data of cement material (e.g., free-lime) is obtained in a short time using a one-dimensional silicon strip detector without the need for component variation. The collaboration sample holder using a pressed sample can be analyzed by both benchtop XRD and XRF instruments without separate sample preparations. Superior quantification results of the four major components are obtained by Rietveld refinement combined with the Bogue calculation. XRD is powerful tool for evaluation of cement material in addition to XRF.

References

(1) R. M. Pulselli, E. Simoncini, R. Ridolfi and S. Bastianoni: *Ecol. Indicators*, **8** (2008), 647–656.
(2) M. F. Ba, C. X. Qian and Y. Zhuang: *Constr. Build. Mater.*, **29** (2012), 438–443.
(3) C. P. Yang: *Eng. Geol.*, **75** (2004), 1–14.
(4) J. Gebauer and A. B. Harnik: *Cement Concr. Res.*, **5** (1975), 163–170.
(5) Introduction to Cement & Concrete: Issued by Japan Cement Association (2009).
(6) A. Ghose and P. Barnes: *Cement Concr. Res.*, **9** (1979), 747–755.
(7) R. H. Bogue: *Ind. Eng. Chem.*, **1** (1929), 192–197.
(8) H. Homma: *Rigaku Journal (English version)*, **35** (2019), 17–23.
(9) ASTM C-114-18, *Standard Test Methods for Chemical Analysis of Hydraulic Cement*.
(10) A. Ohbuchi, T. Konya and G. Fujinawa: *Pow. Diffr.*, **28** (2013), 233–237.
(11) H. M. Rietveld: *J. Applied Cryst.*, **2** (1969), 65–71.
(12) H. Toraya: *J. Appl. Cryst.*, **23** (1990), 485–491.
(13) A. Ohbuchi, Y. Yamada, H. Asakura, I. Tomatsu and M. Murata: *J. Tech. Assoc. Refract. Jpn*, **35** (2015), 250–256.
(14) A. G. De La Torre, S. Bruque and M. A. G. Aranda: *J Applied Cryst.*, **34** (2001), 196–202.
(15) A. Ohbuchi, T. Kuzumaki and T. Nakamura: *Bunseki Kagaku*, **68** (2019), 609–614.
(16) F. H. Chung and R. W. Scott: *J. Appl. Crystallogr.*, **6** (1973), 225–230.
(17) W. A. Dollase: *J. Appl. Cryst.*, **19** (1986), 267–272.
(18) Determination Method for Free lime in Cement, JCAS I-01: Issued by Japan Cement Association (1997).
(19) M. Watanabe: *Rigaku Journal*, **50** (2019), 10–11.
(20) A. Ohbuchi: *Inter. Cement Review*, (2014), 57–60.